Practical Considerations for Generation of Multi-Compartment Complex Coacervates

3.1 Abstract

We discuss preparation of experimental models for multicompartment membraneless organelles in which distinct compositions are maintained indefinitely for macromolecule-rich phases in contact with each other. These model systems are based on the physical chemistry phenomenon of complex coacervation. In complex coacervation, liquid-liquid phase separation occurs due to ion pairing interactions between oppositely-charged polyelectrolytes. This mechanism can drive the associative phase separation of proteins and nucleic acids, the major macromolecular components of membraneless organelles. Here we provide examples, advice and practical considerations for the design, generation, and analysis of multi-compartment complex coacervates. These structures are of interest to compartmentalize the interior of artificial cells and as models for the intracellular membraneless organelles of biological cells.

Keywords: Intracellular condensate, liquid-liquid phase separation, partitioning, compartmentalization, artificial cell

3.2 Introduction

A number of non-membranous intracellular organelles form via liquid-liquid phase separation (LLPS) of their biomacromolecular components (typically nucleic acid and/or protein). Multiple types of intermolecular interactions including charge-charge, cation-π, dipole-

dipole, and π-π stacking can contribute to the associative phase separation process.[1] The resulting intracellular condensates can have varying degrees of fluidity, with some exhibiting more liquidlike and others more gel- or solidlike apparent viscosities.[2-3] Abnormalities are associated with a range of diseases including Alzheimer's disease, ALS, and type 2 diabetes.[1, 4] Multiple types of membraneless organelles, with different biomolecular compositions and functions, exist simultaneously in both the nucleoplasm and cytoplasm of eukaryotic cells. Some intracellular condensates occur as directly contacting subcompartments with characteristic compositions. For example, the multiple subcompartments of the nucleolus have been identified as immiscible liquid phases.[5] Intracellular compartmentalization by numerous distinct membraneless organelles is increasingly appreciated as an important mechanism by which the rich biochemistry of living cells is organized. The complexity of these intracellular condensates *in vivo* makes model systems appealing as a means of studying the underlying principles that influence their properties. Relatively simpler compartments formed by LLPS are also appealing as a means to organize and increase functionality of artificial cells[6] and bioreactors[7-9].

Experimental model systems for biomacromolecular phase separation generally focus on associative phase separation, also called coacervation, which leads one phase rich in macromolecules (termed the coacervate phase) and another, usually much larger volume phase that is comparatively dilute (often called the dilute phase or equilibrium liquid).[10] In general, the liquidlike properties of coacervates are due to the existence of numerous weak, dynamic interactions between components; when intermolecular associations become too strong, gel-like or solid condensates result.[11] Coacervation can be driven by different types of intermolecular interactions, and it is important to understand the intermolecular interactions that lead to phase separation for a particular molecular system in order to design approaches for multiphase

coexistence. For example, elastin-like polypeptides (ELPs) are a well-known phase separating system in which temperature-driven phase separation results from changes in solvation.[12-13] By tuning the hydrophobicity of pentapeptide repeat sequences, Chilkoti, Lopez and coworkers demonstrated control over the critical temperatures for phase separation and were able to generate multiphase, nested droplets with multiple phases formed from different sequences of ELPs.[14-15] For many intracellular condensates that form due to associations of intrinsically disordered proteins and RNAs, charge-charge interactions between the molecular components are important.[16-17] These membraneless compartments can be modeled by a type of phase coexistence called complex coacervation (Figure 1).[11, 18-21]

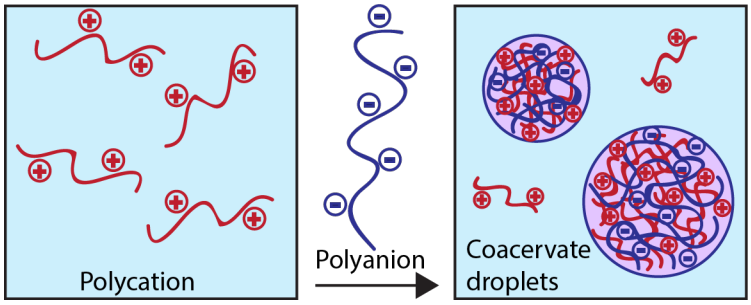

Figure 1: Oppositely charged polyelectrolytes in solution can undergo an associative phase separation event known as complex coacervation resulting in aqueous polymer-rich droplets and a polymer-poor dilute phase. Counterions and solvent water molecules, which are not shown here, are also important to the physical chemistry of the phase separation process.

Complex coacervate systems refer to those driven by ion pairing interactions between oppositely-charged polyions ("complexation"), and the concomitant entropy gain associated with release of counterions.[18] These polyelectrolyte complexes can exist in solution, or phase-separate into a dense, polyelectrolyte-rich liquid coacervate phase or a solid precipitate depending on the relative strength of the intermolecular interactions.[11] Multiphase complex coacervate coexistence with two or more distinct dense, polymer-rich phases, was recently demonstrated by several

groups and provides new models for these coexisting liquid organelles in biology.[22-24] The polyelectrolytes used in these model systems for membraneless organelles have fewer interaction types than are seen in biological systems, as this allows for more straightforward interpretation of physical phenomena. Even so, as biomacromolecules such as polypeptides and nucleic acids are employed, the fundamental interaction types go beyond ion pairing. For example, poly(arginine) contains positively charged guanidinium groups that also have the capacity to participate in cation-π and π-π stacking interactions with the nucleic acid bases, or with the amino acids phenylalanine, tyrosine, and tryptophan.[23, 25-27] Our lab has recently employed complex coacervate systems to generate coexisting compartments using synthetic and biologically inspired polylelectrolytes which show tunable partitioning behavior based on composition.[22] Here we detail protocols and practical considerations for creating multicompartment liquid phase separated polymer systems based on complex coacervation.

3.3 Procedure

The following sections will provide context and specific examples to use as a guide in designing multiphase coacervate systems. They are intended as a starting point for readers to adapt to their own experimental requirements based on their scientific goals. We begin with a discussion of why and how the polyions and solution condition should be pre-tested pairwise to understand likely outcomes upon mixing the full set, and then describe procedures for turbidity measurements, preparation protocols that include three-polyion and four-polyion multiphase coacervate systems, methods for avoiding formation of solid condensates, and considerations for measuring the partitioning of fluorescently-labeled probe molecules across the multiphase coacervate systems.

3.3.1 Screening Coacervate Systems Individually Prior to Multi-Coacervate Formation

Successful design of a multiphase coacervate system requires knowledge of how the component molecules interact in all of their possible combinations. Characteristics of the polyelectrolytes such as multivalency and charge density are important in determining their interaction strength and phase separation behavior.[28-30] The phenomenon of complex coacervation is also dependent on a number of factors including ionic strength, pH, and polyelectrolyte concentration.[18, 31] These factors can be used to tune the interaction strength between polyelectrolytes to optimize the behavior of the overall multiphase system. A charge matching condition of 1:1 cationic:anionic moieties is usually a good starting point for determining relative amounts of the oppositely-charged polyions, particularly for polyelectrolytes with similar multivalency. When multivalencies are mismatched, excess of the smaller polyion may be needed to drive coacervation; an example is the spermidine/polyU RNA system.[32]

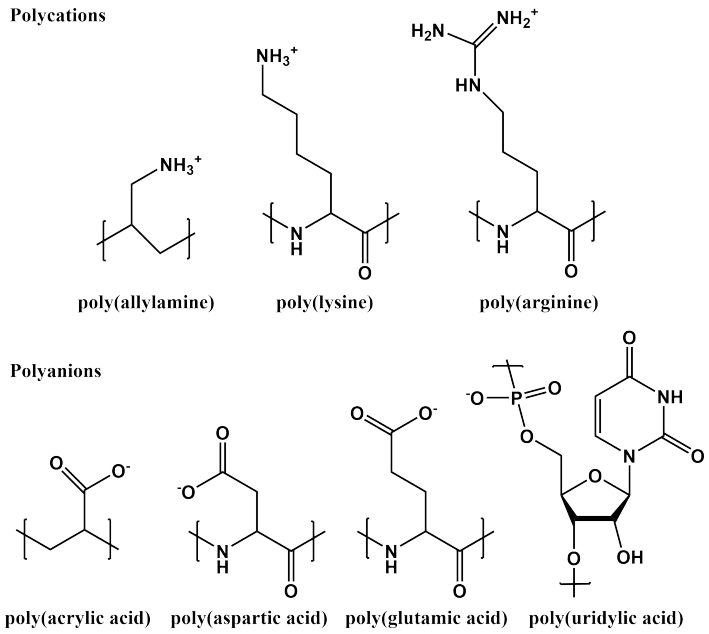

Figure 2: Monomer chemical structure of several polyelectrolytes for complex coacervate experiments, including both synthetic and biologically inspired monomers.

Table 1. Properties of Several Polyelectrolytes Used to Prepare Coexisting Complex Coacervate Systems

Polyelectrolyte	*Abbrev.*	*Molecular Weight (g/mol)*	*Charge/Molecule*	*Mass Per Charge (g/mol)*
RRASLRRASL	2xRRASL	1,185	(+) 4	296
Protamine sulfate[b]	Prot	4,236[a]	(+) 21	202
Poly(L-lysine)	Lys20	3,300 [a]	(+) 20	160
	Lys100	16,000[a]	(+) 100	160
Poly(allylamine hydrochloride)	PAH	17,500[a]	(+) 300	58
Poly(acrylic acid)	PAA	1,800[a]	(-) 25	72
Poly(L-glutamic acid)	Glu100	15,000[a]	(-) 100	150
Poly(L-aspartic acid)[c]	Asp100	14,000[a]	(-) 100	140
Poly(uridylic acid)	polyU	600k - 1,000k[a]	(-) 1850 - 3085	324

[a]Average molecular weight
[b]Protamine is a mixture of naturally occurring arginine rich peptides of similar sequence[33]
[c]Poly(L-aspartic acid) synthesis results in random α-β isomerization of the polymer[34-35]
Reprinted from reference [22] with permission from the American Chemical Society.

We will discuss methods using the set of example polyelectrolytes shown in Figure 2. Abbreviations and chemical properties for these polyelectrolytes are displayed in Table 1. We have found for several different collections of polyelectrolytes that if a given solution environment (i.e., pH, buffer, ionic strength, presence and identity of any divalent metal cations) supports LLPS of two separate pairs of oppositely charged polyelectrolytes, this solution environment will also support coexistence of coacervate phases when all polyelectrolytes are added together.[22] An exception occurs when interactions between any two polyelectrolytes are strong enough to result in gel or solid formation (further discussed in 3.3.4). There are two suggested approaches to screening polymers for use in multi-coacervate systems: (1) with a specific buffer system in mind, for example if physiological pH and ionic strength, or some other particular solution conditions are important or (2) with specific polyelectrolytes in mind. Flexibility in either the solution conditions or the chemical identity of the polyions will generally enable multiphase coacervate systems to be achieved.

Polyelectrolyte pairs are screened for presence of liquid phase separated droplets based on visual presence of turbidity and optical microscopy. Turbidity can be performed rapidly and indicates phase separation but does not differentiate between liquid droplets and solid aggregates. Optical microscopy is used to evaluate whether the resulting complexes are solid, gel-like, or liquid in composition. Generally smooth, spherical microstructures indicate that the material has sufficient fluidity to adopt a surface energy minimizing morphology, although it is possible for solidification to occur after such a morphology has been adopted. Observing droplet coalescence is an excellent way to confirm that structures are in fact liquid, and can be used to monitor changes in phase fluidity.[36-37] Fluorescence recovery after photobleaching (FRAP) of

fluorescently labeled polyelectrolytes or a fluorescently labeled probe molecule can be used to determine the mobility of labeled molecules if desired.[5, 23]

Solid or gel-like morphologies are most likely to be observed between the two polyelectrolytes of a given collection that have the strongest and/or most numerous associative interactions. Therefore, if screening of these "best" oppositely charged polyelectrolytes (i.e., those having the highest charge density and/or number of charges/molecule) results in liquid coacervate formation, non-liquid assemblies are unlikely to be observed in systems where additional polyelectrolytes are also present. In the event that solid formation is observed between the polyelectrolytes that interact most strongly, the solution ionic strength can be increased. However, it is important to consider that coacervates formed from weakly interacting polyelectrolytes may be dissolved by increasing ionic strength. Therefore, knowing the ionic strength range that supports phase separation between the various possible molecular pairings is helpful before manipulating the solution ionic strength. The temperature of the system can also be adjusted in order to tune interaction strengths. Depending on the system, coacervation may display lower critical solution temperature (LCST), upper critical solution temperature (UCST), or both, and adjusting the temperature in a given direction may not have the same effect for all polyelectrolytes.[14-15, 38] We often find it convenient to poise a coacervate system close to a phase transition via tuning one parameter (e.g. ionic strength) so that a small change in another parameter (e.g. temperature) is sufficient to drive the phase transition. Polyelectrolyte concentration can also be increased to encourage phase separation under a given set of solution conditions (ionic strength, pH, temperature); this approach is most useful for systems where one or both polyions has low multivalency.

Table 2: Example of polyelectrolyte screening table for several polyelectrolyte pairings[a, b]

		Charge Concentration (mM)		*Temperature*		
Polycation	*Polyanion*	*polycation*	*polyanion*	*5°C*	*20°C*	*37°C*
Lys20	PAA	5.5	5	L	L	L
Lys20	PolyU	6.88	1.4	L	L	L
Lys100	Asp100	2.5	5	L	L	L
Lys100	PolyU	5	1.4	L	L	L
Lys100	PAA	5	5	S	S	S
Protamine	PAA	4.8	5	L	L	L
2xRRASL	Asp100	4	5	-	-	-
2xRRASL	Glu100	4	5	-	-	-
2xRRASL	PolyU	4	1.4	L	L	L
2xRRASL	PAA	4	5	-	-	S
PAH	PAA	3.9	5	L	L	L
PAH	PAA	5.35	8.33	L	L	L
PAH	Asp100	3.9	5	L	L	L
PAH	Glu100	3.9	5	L	L	L
PAH	PolyU	3.9	1.4	S	S	S

[a] All samples in 50 mM HEPES pH 7.4, 25 mM NaCl, 2 mM $MgCl_2$

[b] L = liquid, S = solid, dash = no phase separation observed

Table 3: Polyelectrolyte screening table for higher (physiological) ionic strength[a, b]

		Charge Concentration (mM)		*Temperature*		
Polycation	*Polyanion*	*polycation*	*polyanion*	*5°C*	*20°C*	*37°C*
Lys20	Asp100	5	5	L	L	L
Lys20	PolyU	2	1.38	L	L	L
Lys20	PAA	4	3.33	L	L	L
Lys100	Glu10	10	10	L	L	L
Lys100	Glu20	2	2	-	-	-
Lys100	Glu20	10	10	L	L	L
Lys100	Glu20	20	20	S	S	S
Lys100	Glu100	5	5	S	S	S
Lys100	Asp100	5	5	L	L	L
Lys100	PolyU	2	1.38	L	L	L
Lys100	PAA	4	3.33	S	S	S
3xRRASL	Asp100	5	5	-	-	-
3xRRASL	Asp100	10	10	L	L	L
3xRRASL	PolyU	6	1.38	L	L	L

[a] All samples in 50 mM HEPES pH 7.4, 150 mM NaCl, 2 mM $MgCl_2$

[b] L = liquid, S = solid, dash = no phase separation observed

3.3.1.1 Screening Polyelectrolytes for Phase Separation in a Desired Buffer System

In order to select polymers for multiphase coacervate systems with a particular buffer system in mind, one should screen individual polyelectrolyte pairs for phase separation and construct a small library of possible polymer pairs resulting in coacervation in the desired buffer. Aside from the functional groups of a given polymer, the overall length of the polymer also influences the strength of ion pairing. Thus, the polymer length can be tuned to influence the buffer parameters under which complex coacervation will occur. For instance, Spruijt *et al.* show that the polymer length of polyacrylic acid (PAA) / poly(N,N,-dimethylaminoethyl methacrylate) (PDMAEMA) coacervate has a strong relationship with the critical salt concentration under which coacervation will occur where increasing length of both polymers results in a higher critical salt concentration (higher salt stability).[30] In general increasing the length (multivalency) of polyelectrolytes will result in a higher ionic strength tolerance but may decrease partitioning of small charged molecules as they compete for charged sited on the oppositely charged polyelectrolyte.[22] If a particular peptide or nucleic acid sequence is desired such as the "RRASL" pentapeptide sequence, increasing the number of repeats (i.e.. RRASLRRASL to RRASLRRASLRRASL) will provide higher ionic strength tolerance.[39] In the case of $RRASL_n$ with polyanion poly(uridylic acid), (polyU), addition of one extra RRASL unit from 2xRRASL to 3xRRASL increases the salt tolerance (at which the coacervates dissolve by nearly 4-fold, from 100 mM NaCl with 2xRRASL/polyU to 350 mM NaCl for 3xRRASL/polyU (at 50 mM HEPES pH 7.4, 4 mM $MgCl_2$).[39] Tables 2 and 3 summarize the phase separation screening data for several polyelectrolytes in two different solution media, one a relatively low ionic strength system (Table 2) and one at physiological ionic strength (Table 3). Screening was performed at three temperatures; we observed different screening results for only one of the systems

(2xRRASL/PAA), which formed solids at 37 ºC but had no visible phase separation at the lower temperatures tested. Despite the lack of obvious thermal sensitivity in these datasets, many coacervating systems are known to have temperature dependent phase behavior near room temperature, including for example the spermine/polyU system.[32] Indeed, this system can exhibit phase separation due to LCST in response to the heat from a researcher's fingers touching the eppindorf tube that contains them.[32]

3.3.1.2 Screening Solution Parameters for Phase Separation of Desired Polyelectrolytes

If specific polyelectrolytes are desired, parameters of the buffer system can be screened in order to find conditions that will allow for liquid phase separation of all of the intended polyelectrolyte pairs. Polyelectrolyte complexation can result in liquid coacervate phase, but sufficiently strong interaction strength between polyelectrolytes can also result in gel-like and/or solid complexation.[11] If non-liquid complexation is observed, increasing the ionic strength of the buffer can result in more liquid complexes through additional charge screening of polyelectrolytes. Temperature can also be adjusted in order to reduce interaction strength between polyelectrolytes, bearing in mind that while some LLPS systems exhibit the more intuitive UCSTs, where heating above a critical point results in coacervate dissolution, many LCSTs, where cooling below a critical point results in coacervate dissolution. If your system of interest has an LCST, heating will favor phase separation. In either case, moving closer to the critical temperature point of coacervate dissolution will result in softening of polyelectrolyte interactions and decrease the probability of solid or gel-like complexes. If no coacervation is observed with the desired polyelectrolytes, ensuring that the solution pH is sufficiently far away from the pKa of ionizable groups of the polymers, such that the polyelectrolytes are highly

charged and decreasing the ionic strength of the solution, will increase ion pairing strength of the polyelectrolytes. Note that while we have emphasized relatively rapid screens for whether or not LLPS occurs between particular polymer pairs under particular conditions, it is often useful to more carefully map out the salt, temperature, pH, concentration, and/or cation:anion concentration ratio to more fully understand a given coacervation system.

3.3.2 Turbidity Measurements

High turbidity is observed in response to scattering of light from generation of polymer rich droplets in complex coacervate samples. Measurements of sample turbidity can be made quickly and are helpful in characterizing coacervate systems as the turbidity of a coacervate sample at a set wavelength (here 500 nm) depends on the presence and amount of coacervation in the sample. An alternative wavelength can be used if, for example, molecules within the system have natural absorbance at 500nm; it is important to report the wavelength at which turbidity is measured. The amount of light scattering from a turbid sample depends on many factors from the wavelength of light to the size, shape, and refractive index of the suspended droplets or particles. We caution against overinterpreting turbidity data, since changes in turbidity can arise for multiple reasons. Turbidity is nonetheless a valuable tool in monitoring for the presence of coacervate droplets in a sample. Some precautions should be taken to ensure consistency due to the possibility of changes in coacervate suspensions over time, for example as droplets coalesce and sediment. In our experience, some coacervate samples show rapid decreases in turbidity over time, due to sedimentation, while others form slowly after initial mixing and therefore show increases in turbidity for the first few minutes.

Turbidity is calculated using the % transmittance of the sample at a set wavelength as shown in equation 1.

Equation 1: $$Turbidity = 100 - \%\, transmittance$$

In practice, a low transmittance means that most of the light entering the sample has been scattered due to coacervate droplets or other particulates suspended in the sample. Such samples will appear visibly cloudy. Because settling of droplets can have a large effect on the measured turbidity of a coacervate sample over time, it is imperative to be consistent with the lifetime and handling of the coacervate samples prior to measurement in order to decrease error in replicate measurements. In practice, we typically generate complex coacervate samples, and immediately transfer to a cuvette for turbidity measurement. If the sample is held in the cuvette for an extended period of time, to observe effects of changing temperature for instance, then adequate pipette mixing should be performed prior to each measurement to ensure that settling does not affect the turbidity data. If the sample is held in a cuvette for an extended period of time as measurements are taken (i.e. varying sample temperature), it is recommended to repeat the measurement in both directions (hot to cold, and cold to hot) in order to check for artefacts due to droplet coalescence and settling. Alternatively, several points can be repeated in the middle of the measurement range to ensure that the sample lifetime is not affecting measured results.

Note: Turbidity measurements can also be taken using a microwell plates and a plate reader, which can be useful if you have many samples to run.

3.3.3 Preparation of Coexisting Systems

Multiphase complex coacervates can be made in a number of ways, and the order of polymer addition may in some cases allow additional control over the resulting coacervate system. Double coacervate systems can be made using pairs of oppositely charged polymers (i.e., two polycations + 2 polyanions) or through addition of a single polyelectrolyte to multiple oppositely charged polyelectrolytes. Examples of each are discussed below.

3.3.3.1 Shared Polymer Complex Coacervates

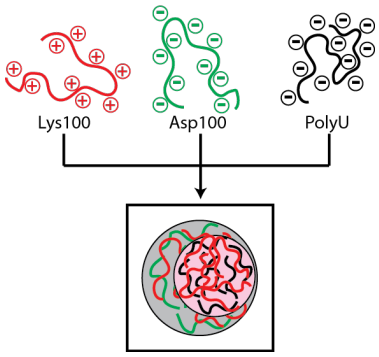

Figure 3: Combining a single polycation (Lys100) with a mixture of polyanions (Asp100, and polyU) at concentrations such that the total charge concentration of polycation to polyanion is approximately 1:1, results in multiphase coacervates that share the polycation. Reprinted from reference [22] with permission from the American Chemical Society.

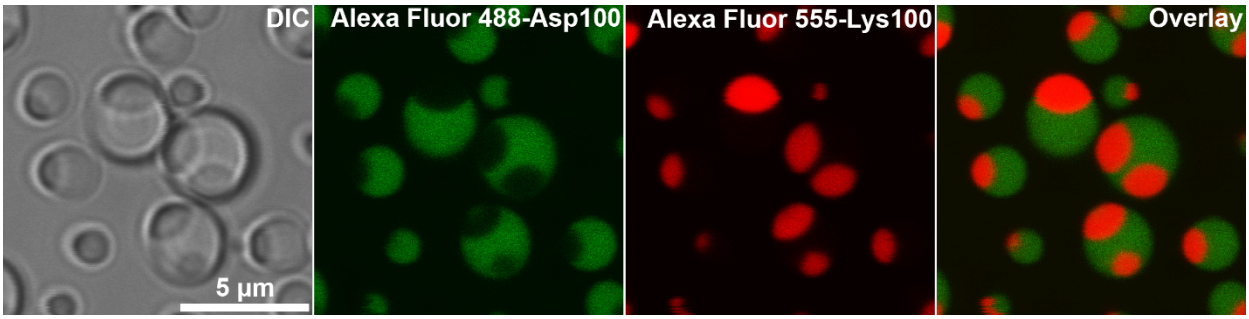

Figure 4: Fluorescence confocal microscopy images of double coacervate system of Lys100, Asp100, and polyU. Individual channels false-colored to indicate which labeled molecule was present and an overlay of fluorescence channels are displayed. Both polyanions (Asp100, polyU) were added simultaneously, followed by the polycation (Lys100). Reprinted from reference [22] with permission from the American Chemical Society.

It is possible to generate coexisting coacervate phases that share a single type of polyion of one sign (e.g. the polycation) and have multiple oppositely-charged polyions (e.g., >1 polyanion) as depicted in Figure 3. For instance, addition of 6.4 mM charge Lys100, and 5 mM charge Asp100 polypeptides to 1.4 mM charge polyU RNA (n= ~2500) results in two distinct coacervate phases that share Lys100 as a common polycation (Figure 4).[6] When generating these kind of shared polymer coacervate systems the order of addition does not appear to affect the resulting coacervates as much as for systems having multiple polycations and multiple polyanions, where metastable complexes may need to be disrupted for equilibrium to be reached. In practice, we premix like-charged polyelectrolytes to addition of oppositely charged polyelectrolytes (i.e. polyanions Asp100, and polyU are premixed prior to addition of polycation Lys100). It seems likely that more than two coexisting coacervate phases could be generated using this type of shared polymer system by including additional polyions (in this example, a third or fourth polyanion). Practical considerations for such efforts include: (1) The total charge concentrations for all polycations should approximately match the total charge concentration for all polyanions. This is to provide sufficient excess polycation to interact with even the least-favorable of the multiple polyanions. (2) The resulting coacervate phases must be sufficiently different to form multiple phases. Different lengths of the same polyelectrolytes may not be sufficient to induce multiple coacervate phases to form (i.e. Lys20 + Lys100 + polyU formed uniform rather than multiphase coacervates in our experiments).[22] (3) The distribution of the shared polyelectrolyte across coacervate phases will reflect the relative strength of its ion pairing interactions with other polyelectrolytes of the system. Within the Lys100, Asp100, polyU system shown in Figure 4 we observe a much higher magnitude of Lys100 in the polyU phase (red, due

to high labeled Lys100 signal) than in the Asp100 phase (green, due to labeled Asp100 signal). Although there is some Lys100 present even in the Asp100-rich phase, the PolyU used in these experiments is comparatively a much longer, more multivalent, polyelectrolyte than Asp100. Polyelectrolyte characteristics such as multivalency and charge density will tune the resulting polymer distributions observed in these shared coacervate systems.[22] Below we detail the procedure for preparing the multiphase coacervates shown in Figures 3 and 4. Both systems correspond to the buffer condition of Table 2.

Materials:

1. 500 mM HEPES, pH 7.4
2. 1 M NaCl
3. 50 mM $MgCl_2$
4. 500 mM charge Aspartic acid sodium salt (n=100, Alamanda Polymers), (Asp 100) in dI water (spiked with ~1% fluorescently labeled Asp 100)
5. 500 mM charge Lysine hydrochloride salt (n=100, Alamanda Polymers), (Lys100) in dI water (spiked with ~1% fluorescently labeled Lys100)
6. 145 mM charge Polyuridylic acid potassium salt, (polyU, 600-1000 kDa, Sigma-Aldrich) in dI water
7. #1.5 glass coverslips
8. 0.12 mm x 9 mm adhesive spacers (secure-seal, Life Technologies)

Note: Concentrations are given in mM charge. This is done because for complex coacervation, ion pairing drives the intermolecular interactions and hence is more readily interpreted than

molarity for polyions of varying size and charge density. Charge concentration is equal to molar concentration multiplied by the net charge of the molecule at the systems pH.

Note: Fluorescently-labeled peptides are prepared as described in section 3.3.5.1.

Note: The coacervate phase may wet the glass coverslip such that droplets are greatly deformed by spreading, or even form a uniform film over the entire surface. Coverslips can be silanized to reduce wetting, for example using an organosilane with a "nonstick" terminal moiety. To silanize, first clean the slides by base treatment (e.g., saturated KOH in isopropanol for 30 min). React clean, dry slides with a toluene solution of 3 mg/mL N-(triethoxysilylpropyl)-O-polyethylene oxide urethane for 4 h, rinse and dry before use.[22]

Procedure:

For a final sample volume of 250 µL with final concentrations of 50 mM HEPES pH 7.4, 25 mM NaCl, 2 mM $MgCl_2$, 6.4 mM charge Lys100, 5 mM charge Asp100, and 1.4 mM charge polyU

1. Add 200.6 µL of dI water, 25 µL of 500 mM HEPES buffer, 6.25 µL of 1 M NaCl, and 10 µL of 50 mM $MgCl_2$ solutions to the centrifuge tube and vortex to mix
2. Add 2.41 µL poly(uridylic acid) and 2.5 µL 500 mM charge poly(aspartic acid) (n=100, Alamanda Polymers) then vortex to mix

3. Add 3.2 µL of 500 mM charge poly(lysine) (n=100, Alamanda Polymers) and mix the solution by gentle pipetting.
4. Immediately seal ~8 µL between two # 1.5 glass coverslips using a 0.12 mm x 9 mm adhesive spacer to prevent evaporation.
5. Wait approximately 15-30 min for droplets to settle to the bottom coverslip and then image using inverted fluorescence or optical microscopy.

3.3.3.2 Pairwise Multiphase Complex Coacervates

Multiphase complex coacervate systems can also be generated from mixtures of multiple polycations and multiple polyanions.[22, 24] Based on screening of individual polyelectrolyte pairs as discussed earlier in Section 3.3.1.1, if liquid phase separation is intended, polymer pairs should be chosen such that no combination of selected polyelectrolytes results in solid formation. Resulting multiphase coacervates will not retain binary pairings of polymer but will instead reach some equilibrium with all present polyelectrolytes in the system determined by the relative interaction strength of polyelectrolytes present (discussed further in section 3.3.5).[22] As a starting point, a charge ratio for each intended polymer pairing should be close to 1:1 (positive to negative charge), with potential optimization necessary especially for polyelectrolyte pairs of non-equal length. Like-charged polyelectrolytes can be premixed prior to simultaneous addition of all polycations and all polyanions to the sample (Figure 5A), or added in a stepwise fashion (Figure 5B) with no observable effect on the morphology or composition of the resulting system.[22] Sequential order of addition (Figure 5B) can be used in order to mitigate solid/gel

formation in non-compatible polyelectrolyte systems where one of the potential polyelectrolyte pairings leads to formation of a solid (see Section 3.3.4).

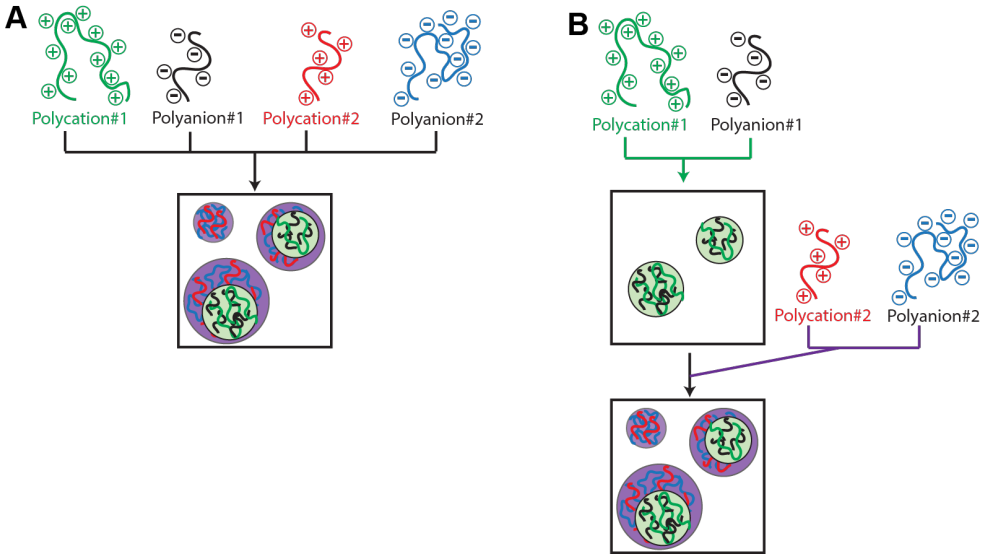

Figure 5: Mixing scheme for coexisting complex coacervate systems: (A) addition of all polyelectrolytes simultaneously by premixing of like-charged polyelectrolytes prior to addition to the sample. (B) polymers are added in pairs, stepwise resulting in generation of one coacervate at a time. Reprinted from reference [22] with permission from the American Chemical Society.

3.3.4 Methods of Overcoming Solid Complexation

In cases where solid formation results from sufficiently strong ion pairing interactions between polyelectrolytes, it is still possible to achieve multi-compartment systems by generating phases in a stepwise fashion (Figure 5B), or by generating the individual coacervates in separate containers prior to mixing the two coacervate systems. In either case it is important to allow some time for equilibration of the initial coacervate phase before introduction of the second coacervate phase components. In practice we find that 3-5 minutes is an appropriate amount of time to allow coacervates to form and equilibrate before addition to a multiphase system, allowing otherwise incompatible polymers to coexist in multi-compartment coacervate systems.

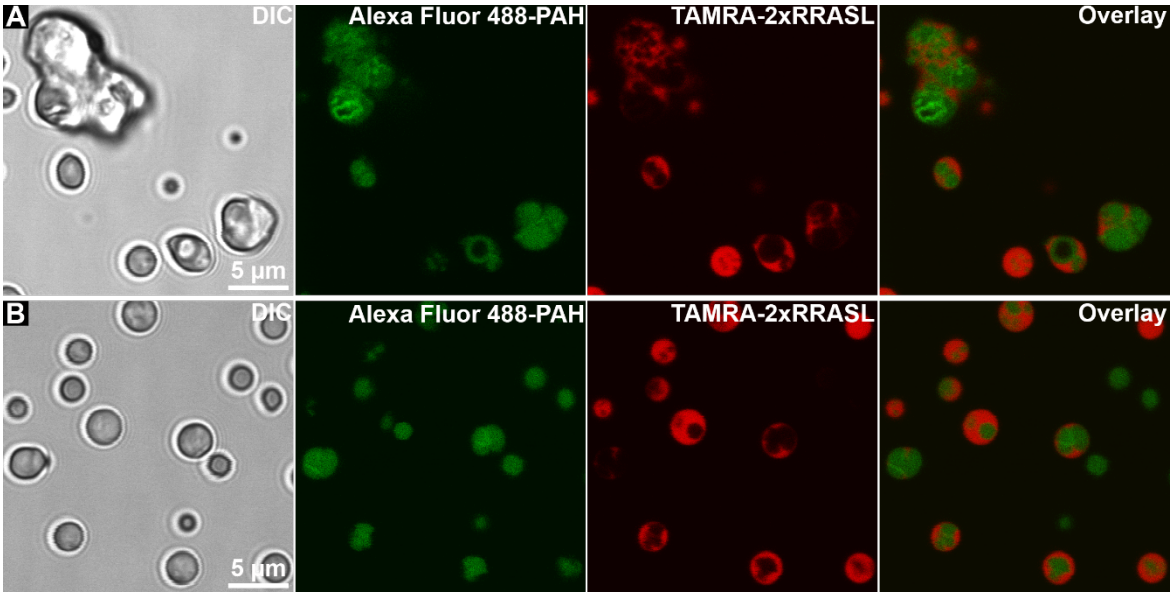

Figure 6: Fluorescence confocal microscopy image of double coacervate system of PAH/PAA and 2xRRASL/polyU. Fluorescently labeled Alexa Fluor 488-PAH (green) and TAMRA-2xRRASL (red) were doped in to aid in visualization of individual phases. Brightness has been enhanced to aid in visualization. (A) Gel-like aggregates of polyelectrolytes are obtained rather than liquid droplets if the order of addition of polyelectrolytes is not controlled for this set of polyelectrolytes. (B) making each coacervate system in separate tubes and allowing a 3 min equilibration period before mixing reduces the occurrence of aggregate like assemblies.

This is demonstrated in systems containing PAH, PAA, RRASLRRASL peptide, and polyU, where PAH and polyU will undergo solid complexation if no control is placed over order of addition for the system due to strong ion pairing interactions (Figure 6A). Generation of each coacervate phase in a stepwise manner results in more spherical coacervate droplets and greatly reduced presence of large aggregated solids (Figure 6B). However, it is important to note that although these systems are metastable for more than 3 days, introducing sheer force through vigorous pipette or vortex mixing will result in solid aggregates. Here, this is likely due to the PAH and polyU gaining access to each other, but may also arise in part from the effect of shear force itself on the interactions between polyelectrolytes. Shear-induced change in physical properties has been observed in comparisons of droplets produced in microfluidic channels vs

free solution,[40] and has now been well characterized across a range of biomolecular condensate compositions in a recent report from Knowles and coworkers.[41]

Materials:

1. 500 mM HEPES, pH 7.4
2. 1 M NaCl
3. 50 mM $MgCl_2$
4. (278 mM charge) poly(acrylic acid), 1.8kDa in dI water
5. (214 mM charge) poly(allylamine hydrochloride, 17.5kDa, (PAH) in dI water (spiked with ~1% Alexa Fluor-488 fluorescently labeled PAH (17.5 kDa)
6. 40 mM charge RRASLRRASL peptide (Genscript, spiked with ~1% TAMRA labeled RRASLRRASL)
7. 145 mM charge poly(uridylic acid potassium salt), (polyU, 600-1000 kDa, Sigma-Aldrich) in dI water
8. #1.5 glass coverslips
9. 0.12 mm x 9 mm adhesive spacers (secure-seal, Life Technologies)

Note: The coacervate phase may wet the glass coverslip such that droplets are greatly deformed by spreading, or even form a uniform film over the entire surface. Coverslips can be silanized to reduce wetting, for example using an organosilane with a "nonstick" terminal moiety. To silanize, first clean the slides by base treatment (e.g., KOH in isopropanol for 30 min). React

clean, dry slides with a toluene solution of 3 mg/mL N-(triethoxysilylpropyl)-O-polyethylene oxide urethane for 4 h, rinse and dry before use.[22]

Procedure:

Two separate samples will be made for (1) 4.03 mM charge PAH and 5.0 mM charge PAA (charge ratio of 0.81, PAH/PAA) and (2) 4 mM charge 2xRRASL and 1.4 mM charge polyU each to a final sample volume of 250 µL each, and final concentrations of 50 mM HEPES pH 7.4, 25 mM NaCl, 2 mM $MgCl_2$. This the buffer condition corresponds to Table 2 screening data.

PAH/PAA coacervate sample

1. Add 199.54 µL of dI water, 25 µL of 500mM HEPES buffer, 6.25 µL of 1 M NaCl, and 10 µL of 50 mM $MgCl_2$ solutions to the centrifuge tube and vortex to mix
2. Add 4.71 µL of 214 mM charge poly(allylamine hydrochloride), (PAH) and vortex to mix
3. 4.5 µL of 278 mM charge poly(acrylic acid), (PAA) and gently pipette mix 2-3 times

2xRRASL/polyU coacervate sample

1. Add 181.34 µL of dI water, 25 µL of 500mM HEPES buffer, 6.25 µL of 1 M NaCl, and 10 µL of 50 mM $MgCl_2$ solutions to the centrifuge tube and vortex to mix
2. Add 25 µL of 40 mM charge 2xRRASL and vortex to mix

3. Add 2.41 µL of 145 mM poly(uridylic acid), (polyU) and gently pipette mix 2-3 times

Generating double-coacervate sample

1. Place 100 µL of each coacervate system into a third tube and gently pipette mix 2-3 times
2. Immediately seal ~8 µL of mixed sample between two # 1.5 glass coverslips using a 0.12mm x 9 mm adhesive spacer to prevent evaporation.
3. Wait approximately 15-30min for droplets to settle to the bottom coverslip and then image using inverted fluorescence or optical microscopy.

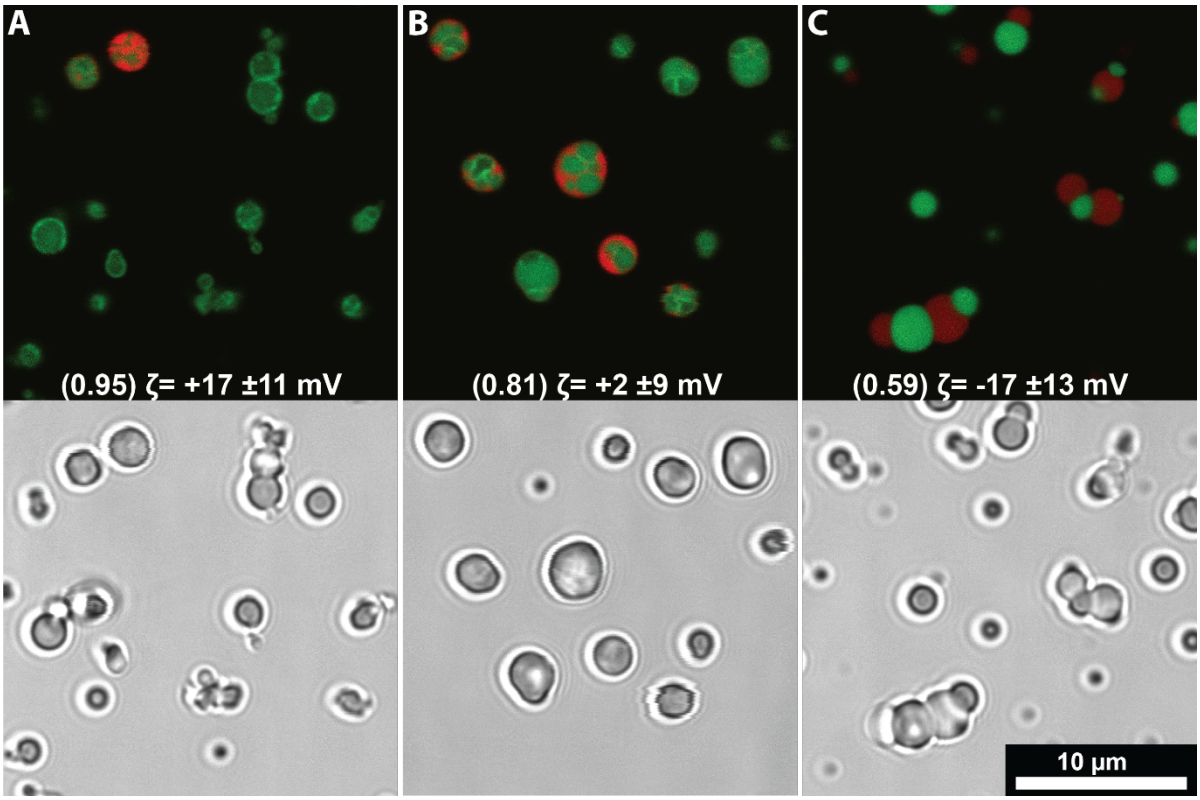

Figure 7: The characteristics of interactions between two unique coacervate systems can be influenced by altering the charge ratio of the coacervate phase. The charge ratio of 2xRRASL/polyU coacervate system (with TAMRA-2xRRASL, false colored red) is held at 2.9 yielding a surface charge, zeta potential (ζ) = -15 ± 8 mV. The charge ratio of PAH/PAA (with Alexa Fluor 488-PAH, false colored green) is altered which in turn affects the observed zeta potential of the PAH/PAA phase (charge ratio and ζ of the PAH/PAA phase in each case is shown). Fluorescence and DIC channels are shown for each formulation. Error represents the standard deviation in ζ potential of triplicate measurements of separately made samples.

We found that tuning the polyelectrolyte ratios of individual polyelectrolyte pairs can further reduce polyelectrolyte incompatibilities resulting in solid formation. PAH/PAA coacervates at a charge ratio near 1:1 (0.95 - PAH/PAA) exhibit a positive surface charge, measured as zeta potential (ζ) = +17 ± 17 mV. 2xRRASL/polyU coacervates generated at a charge ration of 2.9 (2xRRASL/polyU) exhibit a ζ potential of -15 ± 8 mV. PAH/PAA (ζ = +17 ± 17 mV)and 2xRRASL/polyU coacervates (ζ = -15 ± 8 mV) prepared in separate tubes and mixed following a 3 minute equilibration window (Figure 5A) show some degree of aggregate

formation reminiscent of Figure 6A. Descreasing the charge ratio of the PAH/PAA coacervate system to 0.81 (less cation) shown in Figure 7B shifts the droplet surface charge to near neutral ($\zeta = +2 \pm 9$ mV) although aggregates are still observed when mixing with 2xRRASL/polyU coacervates. Further decreasing the charge ratio of PAH/PAA to 0.59 results in a ζ potential of -17 ± 13 mV which when mixed with 2xRRASL/polyU coacervates (Figure 7C) no longer generates observable aggregate material but instead produces alternating chains of spherical droplets that are observed to be stable for up to 3 days. This droplet chaining may indicate electrostatic repulsion between droplets of the same composition.

3.3.5 Probe Partitioning

The partitioning of solutes in complex coacervate systems depends on the composition of the coacervate phase, and can be at least partially understood in terms of ion pairing interactions between the solute of interest and the coacervate polyelectrolyte components.[22, 32, 39] For example, we found that the partitioning of small oligonucleotide and peptide solute probes into complex coacervate systems depends on: (1) the magnitude of ion pairing interactions between the probe and the oppositely charged polyelectrolyte of the coacervate, which drives accumulation, (2) the ion pairing capability of the coacervates like-charged polyelectrolyte (with respect to the probe), which opposes accumulation, and (3) the availability of specific binding interactions such as Watson-Crick base pairing, which can greatly increase solute partitioning into coacervates.[22, 32]

When performing partitioning experiments within a singular coacervate phase, the most important issue is ensuring that adequate time is allowed for equilibrium to be reached within the

sample. In practice, this can be difficult when there is a very strong interaction between the probe molecule and the polyelectrolyte polymers of the coacervate system. One way to alleviate this concern is to introduce the fluorescent probe into solution prior to the addition of either polyelectrolyte ensuring an even dispersion of the fluorescent probe prior to induction of coacervation by adding polyelectrolytes to the sample. Additionally, allowing an equilibration time of 30 minutes or more after generation of the coacervate allows for settling of most coacervate droplets for imaging with inverted microscopy. Probe fluorescence intensity is measured in raw fluorescence via confocal microscopy and compared to a standard curve of fluorescent probe in buffer (in the absence of polyelectrolytes) which is serially diluted to create a calibration curve. Because partitioning of some fluorescent probes is so strong (≥1000x), it is important to make sure that the amount of probe added to the sample (typically to final concentration of 0.01-0.1 μM for our samples) is sufficiently small that the fluorescence intensity of the coacervate phase does not surpass the fluorescence intensity of the stock solution of fluorescent probe, such that it is outside the range of the calibration curve. Additionally, be sure that the maximum pixel intensity for the coacervate droplets is below saturation. If too many pixels are saturated the data will not accurately be translated to a concentration value through the calibration curve of fluorescent probe. If necessary, repeat the experiment with a reduced concentration of added probe to bring the fluorescence intensity in the coacervate phase into the range for which a calibration curve can be prepared. Once labeled probe concentrations and microscope settings are appropriate to allow meaningful fluorescence measurements, images of the coacervate sample can be taken. To achieve an accurate representation of the fluorescence intensity of a coacervate sample, a total of 10+ random droplets from the microscopy image are measured for fluorescence intensity and the region measured is slightly smaller than the full area

of the coacervate droplet (to eliminate inconsistencies in fluorescence resulting from curvature at the edge of the droplets. When using a confocal microscope, the slice thickness of the image can be compared to the diameter of the coacervate droplet to yield insight on the curvature of the droplet and the appropriate size of measurement area. All coacervate samples analyzed are prepared in triplicate to obtain a standard deviation for probe concentration in the coacervate phase.

3.3.5.1 Fluorescently Labeling Polyelectrolytes

When working with more than a single pair of polyelectrolytes the composition of the coacervate phase becomes complicated as polyelectrolytes distribute across the multiple coacervate phases based on the comparative properties of the polyelectrolytes involved. One way to probe this behavior is by introducing a small amount of fluorescently tagged polyelectrolyte and observing its relative distribution throughout the sample. Quantification of partitioning coefficients by fluorescence microscopy is often limited by the very low intensity from the dilute phase; this can be addressed by performing bulk fluorescence measurements (i.e. in a small-volume cuvette), which is generally possible due to the relatively large volume of the dilute supernatant phase compared to the coacervate phase. The commercial availability of fluorescently labeled polyelectrolytes is limited. It therefore may be necessary, and will likely be more cost efficient, to fluorescently label polyelectrolytes in-house. We generally choose to use small molecule fluorophores (like rhodamine, fluorescein, or Alexa Fluor® dyes) rather than large macromolecule-based fluorophores like green fluorescent protein (GFP) because their smaller size (in terms of molecular weight) minimizes impact on the net molecular properties of the molecule, and hence minimizes any difference in its partitioning compared to that of the

unlabeled polyelectrolyte. For the same reason, labels on higher-molecular weight polyelectrolytes are considered less perturbative than those on smaller molecular weight polyions, where the label consequently makes up a larger fraction of the overall labeled molecule and can have a larger impact on its behavior. For low molecular weight solutes, radioisotope labeling can be a good option that avoids changing the solute chemistry and allows quantification over a very large dynamic range;[7, 42] drawbacks include the inability to perform while imaging and the need for careful attention safety considerations.

Longer wavelength dyes (i.e. Alexa Fluor 647 vs Alexa Fluor 488) typically have a large extinction coefficient allowing for greater signal at lower degrees of labeling. A variety of reactive fluorescent dyes can be purchased with specific reactivity for chemical functional groups such as primary amines, and carboxylic acid groups which are common in polyelectrolyte systems. These reactive dyes typically come with detailed manufacturer suggested protocols for labeling. For instance, labeling of primary amine containing polyelectrolytes with N-succinimidyl (NHS) ester functionalized reactive dyes selectively reacts with primary amine groups of polyelectrolytes and forms a stable amide bond between the amine containing molecule and the dye as shown in Figure 8.

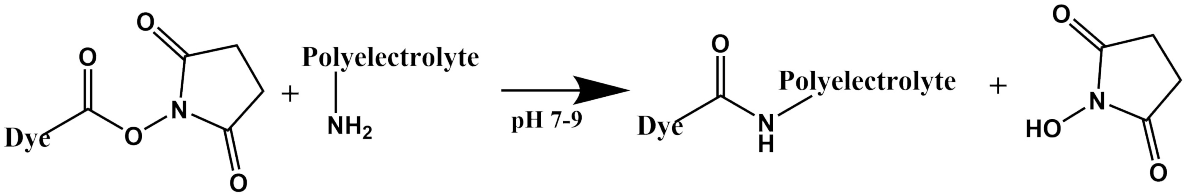

Figure 8: Reaction scheme of N-succinimidyl ester reactive dyes with primary amine containing molecules results in stable amide bond formation between the dye and polyelectrolyte. The reaction relies on the primary amine containing molecule to act as a nucleophile, therefore an elevated pH (pH: 7-9) is required for efficient conjugation.

3.3.5.2 Purification of Fluorescently Labeled Polyelectrolytes

Small charged molecules, such as unreacted dyes remaining after polyelectrolyte labeling reactions, can be expected to partition differently than the labeled polyelectrolytes.[22, 32, 39, 43] Therefore, it is very important to ensure that all unreacted dye remaining from polyelectrolyte labeling has been removed. Several premanufactured options exist for purification of fluorescently labeled macromolecules such as Zebra™ desalting columns (Thermo Fischer Scientific) at various molecular weight cutoff points. In our experience, superior purification was achieved at the cost of convenience by using conventional glass columns packed with size exclusion purification resin, such as GE Healthcare Life Sciences Sephadex® resins, or Bio-Rad Laboratories Bio-Gel® resins. Various size exclusion ranges are available for these options and can be selected is such a way that the labeled polyelectrolyte is quickly and easily separated from the unreacted dye so long as the polyelectrolyte molecular weight is sufficiently larger than the dye molecular weight. For example, Figure 9 shows a purification of Alexa Fluor 546 labeled poly(L-lysine) reaction mixture using Bio-Rad Bio-Gel® P-4 resin. Alexa Fluor 546-NHS ester has a molecular weight of 1,159.6 g/mol, and poly(L-lysine) n=100 has an average molecular weight of 16,000 g/mol. Employing Bio-Rad Bio-Gel® P-4 resin with a size exclusion range of 800-4,000 g/mol allows the functionalized Lys100 flow quickly though the column separating it from the unreacted dye flows which falls within the size exclusion range of the resin and travels much more slowly. The column diameter can be modified to suit different scale labeling reactions (i.e. larger labeling volumes would require a larger diameter column for optimum separation and reduced sample dilution), and the column bed volume can be modified to achieve better separation and minimize sample dilution (i.e. a larger bed volume would increase separation at the cost of increased sample dilution as the sample band broadens over time).

Figure 9: Purification of Alexa Fluor® 546-NHS ester labeling of Lys100 using Bio-Gel® P4 size exclusion resin. The faster moving pink band (bottom) corresponds to functionalized Lys100 which is separated from unfunctionalized dye (slower moving pink band (top), and can be collected as it elutes from the column.

3.3.5.3 Importance of Avoiding Overlabeling

Finally, one of the most important practical consideration when fluorescently labeling molecules is that the change in net charge and molecular weight of the resulting labeled macromolecule or polyelectrolyte should be sufficiently small as to preserve the physical and chemical characteristics of the polymer. Over-labeling of polyelectrolytes with dye moieties can alter their partitioning and phase behavior. For example, introducing fluorescently labeled Lys100 with a theoretical degree of labeling (DOL) of ~20 dyes per polymer using Alexa Fluor 555-NHS ester into a coacervate system of unlabeled 5 mM charge Lys100 and 5 mM charge Asp100 results in a low level of diffuse fluorescence throughout the coacervate droplets and formation of highly fluorescent puncta within coacervate droplets (Figure 10A). Labeled Lys100 accounts for approximately 1% of the total Lys100 in the sample. It turns out these puncta are the

result of the overlabeled Lys100, which behaves as a chemically distinct species and drives formation of a new phase. Labeled and unlabeled Lys100 molecules may interact differently with the polyanion and/or intramolecular interactions between the negatively charged Alexa Fluor dye and the remaining unreacted Lys sidechains could be effectively generating an amphiphilic molecule as a result of over-labeling. Reducing the theoretical DOL from 20 to 10 does not eliminate puncta but does result in increased diffuse fluorescence throughout the coacervate droplets (Figure 10B). Reducing the theoretical DOL further to 3 dyes per polymer of Lys100 eliminates puncta formation and results in homogenous fluorescence throughout the coacervate droplet (Figure 10C). In practice, the DOL should be minimized to avoid any change in polymer characteristics, typically a DOL of 1-3% of monomers yields sufficient fluorescence signal. Using fluorophores with higher extinction coefficients like Alexa Fluor 647 (ε= 270,000 $cm^{-1}M^{-1}$) allows for lower DOL while retaining high fluorescence signal.

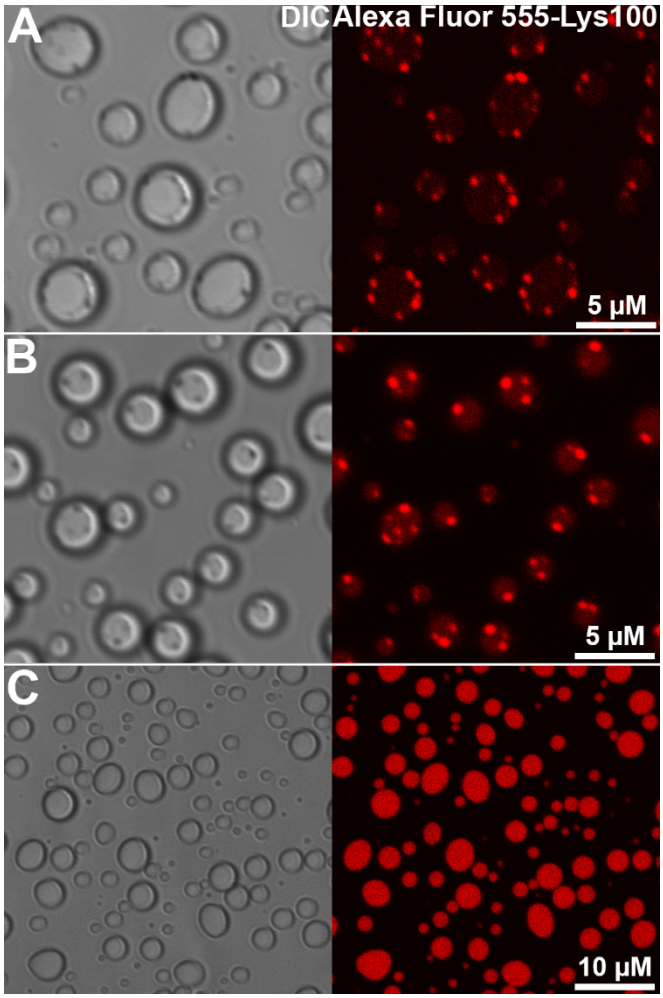

Figure 10: Coacervates composed of 5 mM charge Lys100 and 5 mM charge Asp100 with added Alexa Fluor 555 labeled Lys100 accounting for approximately 1% of the total Lys100 concentration at the following theoretical degrees of labeling: A) 20 labels per molecule, B) 10 labels per molecule, and C) 3 labels per molecule.

3.4 Acknowledgments

This work was supported by the National Science Foundation, grant MCB-1715984. The authors thank Jacob Shaffer for helpful comments on the manuscript.

3.5 References

1. Brangwynne, Clifford P.; Tompa, P.; Pappu, Rohit V., Polymer physics of intracellular phase transitions. *Nature Physics* **2015,** *11*, 899.
2. Hyman, A. A.; Weber, C. A.; Julicher, F., Liquid-liquid phase separation in biology. *Annu Rev Cell Dev Biol* **2014,** *30*, 39-58.
3. Mitrea, D. M.; Kriwacki, R. W., Phase separation in biology; functional organization of a higher order. *Cell Communication and Signaling* **2016,** *14* (1), 1-20.
4. Shin, Y.; Brangwynne, C. P., Liquid phase condensation in cell physiology and disease. *Science* **2017,** *357* (6357), eaaf4382.
5. Feric, M.; Vaidya, N.; Harmon, Tyler S.; Mitrea, Diana M.; Zhu, L.; Richardson, Tiffany M.; Kriwacki, Richard W.; Pappu, Rohit V.; Brangwynne, Clifford P., Coexisting Liquid Phases Underlie Nucleolar Subcompartments. *Cell* **2016,** (165), 1686-1697.
6. Crowe, C. D.; Keating, C. D., Liquid-liquid phase separation in artificial cells. *Interface Focus* **2018,** *8* (5), 20180032.
7. Dewey, D. C.; Strulson, C. A.; Cacace, D. N.; Bevilacqua, P. C.; Keating, C. D., Bioreactor droplets from liposome-stabilized all-aqueous emulsions. *Nature Communications* **2014,** *5*, 4670.
8. Rowland, A. T.; Cacace, D. N.; Pulati, N.; Gulley, M. L.; Keating, C. D., Bioinspired Mineralizing Microenvironments Generated by Liquid–Liquid Phase Coexistence. *Chem Mater* **2019,** *31* (24), 10243-10255.
9. Nakashima, K. K.; Vibhute, M. A.; Spruijt, E., Biomolecular Chemistry in Liquid Phase Separated Compartments. *Frontiers in Molecular Biosciences* **2019,** *6* (21).
10. Aumiller, W. M., Jr.; Davis, B. W.; Keating, C. D., Phase separation as a possible means of nuclear compartmentalization. *Int Rev Cell Mol Biol* **2014,** *307*, 109-49.
11. Wang, Q.; Schlenoff, J. B., The Polyelectrolyte Complex/Coacervate Continuum. *Macromolecules* **2014,** *47* (9), 3108-3116.
12. MacEwan, S. R.; Chilkoti, A., Elastin-like polypeptides: Biomedical applications of tunable biopolymers. *Peptide Science* **2010,** *94* (1), 60-77.
13. Wang, R.; Ozsvar, J.; Yeo, G. C.; Weiss, A. S., Hierarchical assembly of elastin materials. *Current Opinion in Chemical Engineering* **2019,** *24*, 54-60.
14. Quiroz, F. G.; Chilkoti, A., Sequence heuristics to encode phase behaviour in intrinsically disordered protein polymers. *Nat Mater* **2015,** *14* (11), 1164-1171.
15. Simon, J. R.; Carroll, N. J.; Rubinstein, M.; Chilkoti, A.; Lopez, G. P., Programming molecular self-assembly of intrinsically disordered proteins containing sequences of low complexity. *Nat Chem* **2017,** *9* (6), 509-515.
16. Dignon, G. L.; Best, R. B.; Mittal, J., Biomolecular Phase Separation: From Molecular Driving Forces to Macroscopic Properties. *Annual Review of Physical Chemistry* **2020,** *71* (1), 53-75.
17. Brangwynne, C. P.; Tompa, P.; Pappu, R. V., Polymer physics of intracellular phase transitions. *Nat Physics* **2015,** *11*.
18. Bungenberg de Jong, H. G., Complex Colloid Systems. In *Colloid Science*, Kruyt, H. R., Ed. Elsevier: Amsterdam, 1949; Vol. II, pp 335-432.
19. Gucht, J. v. d.; Spruijt, E.; Lemmers, M.; Cohen Stuart, M. A., Polyelectrolyte complexes: Bulk phases and colloidal systems. *Journal of Colloid and Interface Science* **2011,** *361* (2), 407-422.
20. Perry, S. L., Phase separation: Bridging polymer physics and biology. *Current Opinion in Colloid & Interface Science* **2019,** *39*, 86-97.

21. Bungenberg de Jong, H. G.; Kruyt, H. R., Coacervation (partial miscibility on colloid systems) (preliminary communication). *Proc. Royal Acad. Amsterdam* **1929,** *32*, 849-856.
22. Mountain, G. A.; Keating, C. D., Formation of Multiphase Complex Coacervates and Partitioning of Biomolecules within them. *Biomacromolecules* **2019,** *21* (2), 630-640.
23. Boeynaems, S.; Holehouse, A. S.; Weinhardt, V.; Kovacs, D.; Van Lindt, J.; Larabell, C.; Van Den Bosch, L.; Das, R.; Tompa, P. S.; Pappu, R. V.; Gitler, A. D., Spontaneous driving forces give rise to protein−RNA condensates with coexisting phases and complex material properties. *Proceedings of the National Academy of Sciences of the United States of America* **2019,** *116* (16), 7889.
24. Lu, T.; Spruijt, E., Multiphase Complex Coacervate Droplets. *Journal of the American Chemical Society* **2020**.
25. Tatko, C. D.; Waters, M. L., The geometry and efficacy of cation–π interactions in a diagonal position of a designed β-hairpin. *Protein Science* **2003,** *12* (11), 2443-2452.
26. Hughes, R. M.; Waters, M. L., Arginine Methylation in a β-Hairpin Peptide: Implications for Arg−π Interactions, ΔCp°, and the Cold Denatured State. *Journal of the American Chemical Society* **2006,** *128* (39), 12735-12742.
27. Beaver, J. E.; Waters, M. L., Molecular Recognition of Lys and Arg Methylation. *Acs Chem Biol* **2016,** *11* (3), 643-653.
28. Choi, J.-M.; Holehouse, A. S.; Pappu, R. V., Physical Principles Underlying the Complex Biology of Intracellular Phase Transitions. *Annual Review of Biophysics* **2020,** *49* (1), 107-133.
29. Chang, L.-W.; Lytle, T. K.; Radhakrishna, M.; Madinya, J. J.; Vélez, J.; Sing, C. E.; Perry, S. L., Sequence and entropy-based control of complex coacervates. *Nature Communications* **2017,** *8* (1), 1273.
30. Spruijt, E.; Westphal, A. H.; Borst, J. W.; Cohen Stuart, M. A.; van der Gucht, J., Binodal Compositions of Polyelectrolyte Complexes. *Macromolecules* **2010,** *43* (15), 6476-6484.
31. Priftis, D.; Xia, X.; Margossian, K. O.; Perry, S. L.; Leon, L.; Qin, J.; de Pablo, J. J.; Tirrell, M., Ternary, Tunable Polyelectrolyte Complex Fluids Driven by Complex Coacervation. *Macromolecules* **2014,** *47* (9), 3076-3085.
32. Aumiller, W. M.; Cakmak, F. P.; Davis, B. W.; Keating, C. D., RNA-Based Coacervates as a Model for Membraneless Organelles: Formation, Properties, and Interfacial Liposome Assembly. *Langmuir* **2016,** *32* (39), 10042-10053.
33. Hoffmann, J. A.; Chance, R. E.; Johnson, M. G., Purification and analysis of the major components of chum salmon protamine contained in insulin formulations using high-performance liquid chromatography. *Protein Expression and Purification* **1990,** *1* (2), 127-133.
34. Clarke, S., Propensity for spontaneous succinimide formation from aspartyl and asparaginyl residues in cellular proteins. *International Journal of Peptide and Protein Research* **1987,** *30* (6), 808-821.
35. Aswad, D. W.; Paranandi, M. V.; Schurter, B. T., Isoaspartate in peptides and proteins: formation, significance, and analysis. *Journal of Pharmaceutical and Biomedical Analysis* **2000,** *21* (6), 1129-1136.
36. Wang, J.; Choi, J.-M.; Holehouse, A. S.; Lee, H. O.; Zhang, X.; Jahnel, M.; Maharana, S.; Lemaitre, R.; Pozniakovsky, A.; Drechsel, D.; Poser, I.; Pappu, R. V.; Alberti, S.; Hyman, A. A., A Molecular Grammar Governing the Driving Forces for Phase Separation of Prion-like RNA Binding Proteins. *Cell* **2018,** *174* (3), 688-699.e16.
37. Kaur, T.; Alshareedah, I.; Wang, W.; Ngo, J.; Moosa, M. M.; Banerjee, P. R., Molecular Crowding Tunes Material States of Ribonucleoprotein Condensates. *Biomolecules* **2019,** *9* (2).

38. Nott, T. J.; Petsalaki, E.; Farber, P.; Jervis, D.; Fussner, E.; Plochowietz, A.; Craggs, T. D.; Bazett-Jones, D. P.; Pawson, T.; Forman-Kay, J. D.; Baldwin, A. J., Phase Transition of a Disordered Nuage Protein Generates Environmentally Responsive Membraneless Organelles. *Molecular Cell* **2015,** *57* (5), 936-947.
39. Aumiller, W. M.; Keating, C. D., Phosphorylation-mediated RNA/peptide complex coacervation as a model for intracellular liquid organelles. *Nat Chem* **2016,** *8* (2), 129-137.
40. van Swaay, D.; Tang, T.-Y. D.; Mann, S.; de Mello, A., Microfluidic Formation of Membrane-Free Aqueous Coacervate Droplets in Water. *Angewandte Chemie International Edition* **2015,** *54* (29), 8398-8401.
41. Shen, Y.; Ruggeri, F. S.; Vigolo, D.; Kamada, A.; Qamar, S.; Levin, A.; Iserman, C.; Alberti, S.; George-Hyslop, P. S.; Knowles, T. P. J., Biomolecular condensates undergo a generic shear-mediated liquid-to-solid transition. *Nature Nanotechnology* **2020**.
42. Frankel, E. A.; Bevilacqua, P. C.; Keating, C. D., Polyamine/Nucleotide Coacervates Provide Strong Compartmentalization of Mg2+, Nucleotides, and RNA. *Langmuir* **2016,** *32* (8), 2041-2049.
43. Marianelli, A. M.; Miller, B. M.; Keating, C. D., Impact of macromolecular crowding on RNA/spermine complex coacervation and oligonucleotide compartmentalization. *Soft Matter* **2018,** *14* (3), 368-378.